

# Enthalpy and volume relaxation of PMMA, PC, and a-Se: evaluation of aging bulk moduli

Petr Slobodian<sup>a,\*</sup>, Pavel Říha<sup>b</sup>, Anežka Lengálová<sup>a</sup>, Jiří Hadač<sup>a</sup>,  
Petr Sába<sup>a</sup>, Josef Kubát<sup>a,c</sup>

<sup>a</sup> Faculty of Technology, Tomas Bata University in Zlín, Polymer Centre, T.G.M. 275, 762 72 Zlín, Czech Republic

<sup>b</sup> Institute of Hydrodynamics, Academy of Sciences of the Czech Republic, Pod Patankou 3015, 16612 Prague, Czech Republic

<sup>c</sup> Department of Materials Science and Engineering, Chalmers University of Technology, SE-41296 Gothenburg, Sweden

Received 16 February 2004; received in revised form 12 June 2004

Available online 15 September 2004

## Abstract

Enthalpy,  $h$ , and volume,  $v$ , relaxation of poly(methyl methacrylate), PMMA, and polycarbonate, PC, were measured using differential scanning calorimetry and mercury-in-glass dilatometry. For PMMA both temperature down-jumps and up-jumps were studied. Attention was paid to the influence of cooling/heating rates on aging process with the result that it is related to the corresponding shift of glass transition temperature,  $T_g$ . From the time dependence of enthalpy,  $h$ , and volume,  $v$ , the aging modulus was defined as  $K_a = (\partial h / \partial v)_T$ , and was found to be ca. 2 GPa. This corresponds roughly to the inverse value of the compressibility,  $\kappa_1$ , in the vicinity of  $T_g$ . The results of the measurements on amorphous selenium supported the notion that  $K_a$  assumes values close to  $1/\kappa_1$ . The measured  $K_a$  values were about 5 GPa, in fair agreement with compressibility data extracted from  $pVT$  measurements. © 2004 Published by Elsevier B.V.

PACS: 61.20.Lc; 65.60+a; 64.70.Pf

## 1. Introduction

Physical aging is a time-dependent process caused by changes in temperature or pressure within or below the glass transition region. Although aging processes can be observed in a variety of substances [1], it is mainly associated with amorphous polymers, inorganic glasses, and low-molecular glass formers. Basically, physical aging is a slow consolidation of complex molecular structure, accompanied by changes of thermodynamic characteristics [2–4], mechanical properties [1], and other parameters of the material.

The aging process is usually initiated by sudden changes in temperature, either increase (up-jump), or de-

crease (down-jump), and is determined from the changes in enthalpy,  $h$ , and volume,  $v$ . In literature the data on enthalpy and volume relaxation are normally reported separately; the relation between these two quantities has only been discussed in a few instances. The dependence of  $\Delta h$  on  $\Delta v$ , which is fairly linear, gives typically the value of  $\Delta h / \Delta v = 1\text{--}2$  GPa [5–8].

Adachi and Kotaka [5] found this quantity for polystyrene (PS) of about 2 GPa, associating it with the enthalpy of free volume creation. Related to this is also the work of Oleinik [6], who found that in PS aging the process differs for temperature up-jump and down-jump (the former being by 30% higher than the latter). He interpreted the relation  $v = \text{const} \cdot h$  as resulting from a common mechanism underlying both these quantities. The results in the paper form perfectly straight lines with a surprisingly low scatter in both types of experiments, irrespective of the variation in aging temperatures,  $T_a$ ,

\* Corresponding author. Tel.: +420 57 603 1350; fax: +420 57 603 1444.

E-mail address: [slobodian@ft.utb.cz](mailto:slobodian@ft.utb.cz) (P. Slobodian).

or storage time. The value  $\Delta h/\Delta v$  found here is about 1–2 GPa. Simon et al. measured aging of polyetherimide [7] and PS [8] and determined the corresponding values to be 1.8 and 1.2 GPa, respectively. Cowie et al. [9] followed  $h$  and  $v$  relaxation on poly(vinyl acetate); however, in this case no simple correlation between the two quantities was found. In the initial stage the  $\Delta h/\Delta v$  ratio increased, then reached a maximum (at about  $10^2$  min), and finally it decreased to zero at a rate depending on  $T_a$ . As could be seen, no uniform opinion on the relation between  $\Delta h$  and  $\Delta v$  has been accepted yet.

Before ascribing any physical meaning to the ratio of  $\Delta h/\Delta v$ , one has to consider the experimental methods commonly used in determining the aging process. The measurements of volume relaxation may appear simple and straightforward, but they have an inherent weakness caused by relatively long equilibration times. This is due to the rather large sample volumes (several  $\text{cm}^3$ ) normally needed to achieve sufficient accuracy, both in the mercury-in-glass (MIG) method and various thermomechanical devices measuring uniaxial dimensional changes. The result is that the initial part of the volume–time dependence is not known because it takes some time for the sample to get to a constant temperature at which aging is determined; in the beginning stage the aging process cannot be separated from other simultaneous processes.

In enthalpy measurements, normally carried out on DSC devices, the sample is small, typically 10 mg. This reduces the problems associated with the temperature equilibration, but on the other hand, it causes high scatter of the results. Further, in order to obtain a single point in the  $\Delta h$ -time graph a separate measurement is required, which is extremely time demanding. The amount of relaxed or consumed enthalpy is assessed from the changing size of endothermic peaks appearing on the  $c_p$ - $T$  records in the vicinity of glass transition temperature,  $T_g$ . It should be noted that enthalpy changes, whether negative or positive (i.e. resulting from temperature down-jumps or up-jumps) are evaluated from  $T$  up-scans in the DSC device.

The papers discussed above [5–9] do not mention the physical meaning of  $\Delta h/\Delta v$ . In [10] the standard thermodynamics formula

$$K_a \stackrel{\text{irr}}{\leftarrow} \left( \frac{\partial h}{\partial v} \right)_T \stackrel{\text{rev}}{\Rightarrow} \frac{\alpha T}{\kappa} - \frac{1}{\kappa} \quad (1)$$

is used to define, in a purely formal manner, the aging modulus,  $K_a$ , relating to irreversible process of aging. In the equation  $\alpha$  denotes the coefficient of thermal expansion of the material, and  $\kappa$  is compressibility.

In the following we will try to suggest possible physical meaning of the  $\partial h/\partial v$  on the theoretical level. The first treatment of the aging process in terms of irreversible thermodynamics with a single internal variable was

presented by Davies and Jones [11,12]. When replacing the internal variable by a fictive temperature,  $T_f$ , or, alternatively, a fictive pressure  $p_f$ , they arrived at the following relations applying at constant temperature and external pressure:

$$dq = \Delta c_p dT_f, \quad (2)$$

$$dv/v = \Delta \alpha dT_f, \quad (3)$$

$$dq = -vT\Delta \alpha dp_f, \quad (4)$$

$$dv/v = -\Delta \kappa dp_f. \quad (5)$$

Here,  $dq$  denotes the heat exchanged with the surroundings, and  $\Delta c_p$ ,  $\Delta \alpha$ , and  $\Delta \kappa$  are the differences between glass (or frozen-in state) and equilibrium in the heat capacity, thermal expansion, and compressibility, respectively. Eqs. (2)–(5) were derived under the assumption that the system is close to equilibrium and that its behavior can be linearized. The quantity  $dq$  is defined as

$$dq = du + pdv = dh, \quad (6)$$

where  $u$  is the internal energy. The equality  $dq = dh$  results from the standard definitions  $dh = Tds + vdp$  and  $du = Tds - pdv$  when the pressure is kept constant.

When combining Eqs. (2) and (4) with (3) and (5) one obtains

$$\left( \frac{dh}{dv} \right)_{T,p} = \frac{\Delta c_p}{v\Delta \alpha} = T \frac{\Delta \alpha}{\Delta \kappa}. \quad (7)$$

Eq. (7) defines the Prigogine–Defay ratio  $\Pi$

$$\Pi = \frac{\Delta c_p \Delta \kappa}{Tv\Delta \alpha^2} = 1, \quad (8)$$

which also follows from the two Ehrenfest relations describing the pressure dependence of the transition temperature of the second order equilibrium transitions [11,12]. It should be noted that during such transitions the two phases constituting the system in question are in equilibrium. For additional information about the thermodynamic background of  $dT_g/dp$  and the glass-rubber transition the reader is referred to [13,14].

However,  $\Pi$  is often found to differ from 1 (e.g. [15,16]). In Nieuwenhuizen's papers [17,18] an attempt is made to interpret the deviations from  $\Pi = 1$  by introducing a non-equilibrium element in the process in terms of slowly relaxing configurational excess entropy,  $I$ , for the internal energy,  $u$ :

$$du = T ds_{ep} + T_e dI - pdv \quad (9)$$

with  $s_{ep}$  denoting the entropy of the molecular processes taking place at a rate high enough to follow changes in the external variables (equilibrium process),  $I$  the entropy contribution of the slow configurational modes, and  $T_e(t)$  the corresponding effective temperature equal to

the fictive temperature  $T_f$  (tool temperature) mentioned above.

Starting from Eq. (9) we obtain for the change in enthalpy

$$dh = T ds_{ep} + T_c dI + v dp. \quad (10)$$

From Eq. (10) the following expression can be derived for  $(\Delta h/\Delta v)_T$

$$\left(\frac{\partial h}{\partial v}\right)_T = \frac{\alpha T - 1}{\kappa_T} + \frac{1}{v\kappa_T} \left[ T \left(\frac{\partial I}{\partial p}\right)_T \left(\frac{\partial T_c}{\partial T}\right)_p - T \left(\frac{\partial I}{\partial T}\right)_p \left(\frac{\partial T_c}{\partial p}\right)_T - T_c \left(\frac{\partial I}{\partial p}\right)_T \right]. \quad (11)$$

The first rhs term of Eq. (11) corresponds to the standard (reversible) expression of Eq. (1). The correction terms come from the frozen-in configurational entropy,  $I$ , and the effective (fictive) temperature,  $T_c$ . An experimental verification of these terms appears to lie beyond the possibilities of presently available measuring techniques.

In several of his papers Nieuwenhuizen [17,18] briefly mentioned the possibility of extending Eq. (10) by introducing an effective internal pressure,  $p_e$ , equivalent to the fictive pressure,  $p_f$  used in Eqs. (4) and (5) above. As pointed out by Davies and Jones [11,12] this pressure can attain values of several hundred MPa. It can be noted that this pressure is negative when the glass former is cooled below  $T_g$ . When introducing  $p_e$  into Eq. (10) and proceeding in the same manner as in derivation of Eq. (11), one obtains a similarly built equation extended with the terms relating to  $p_e$ . Also in this case the first rhs term is equal to the expression given in Eq. (1). According to Nieuwenhuizen [17,18], theoretical approaches to aging leading to  $\Pi = 1$  cannot provide a reasonable explanation of the experimental facts. This necessarily also extends to methods employing one internal parameter [11,12,19], where  $\Delta h/\Delta v$  is related to the entropic term only. Although Nieuwenhuizen's suggestion to extend Eq. (10) by a work term associated with the dissipation of frozen-in free energy appears highly promising, it is not possible to quantify this idea in such a form that it becomes directly applicable to research results. However,  $\partial h/\partial v$  in the proposed Eq. (11) is inversely proportional to compressibility, which we are going to prove in our paper.

## 2. Experimental

### 2.1. Materials

The following materials were used in this study:

Amorphous poly(methyl methacrylate), a-PMMA, density  $1.19 \text{ g/cm}^3$ ,  $M_w = 90 \text{ kg/mol}$ , mid-point enthalpic

$T_{g,enth.} = 95^\circ\text{C}$ ; the polymer contained 6 mol% methyl acrylate randomly distributed, as determined by  $^{13}\text{C}$  NMR [20].

Polycarbonate, PC, polymer for injection molding of compact discs, density  $1.13 \text{ g/cm}^3$ ,  $T_{g,enth.} = 145^\circ\text{C}$ .

Amorphous selenium, a-Se, of 5N purity, density  $4.24 \text{ g/cm}^3$ ,  $T_{g,enth.} = 38^\circ\text{C}$ , was melted in a glass tube under vacuum at  $300^\circ\text{C}$  for 20h. Thereafter the tube was quenched in room-temperature water. The specimen was adapted to a shape suitable for the mercury-in-glass dilatometry.

### 2.2. Equipment

In the experiments volumetric and enthalpic changes were measured, which were then expressed as  $\Delta h/\Delta v$  and compared with the corresponding material's compressibility.

For *volumetric* measurements mercury-in-glass dilatometry (MIG) according to ASTM Standard D 864-52 was used. The samples were bars of rectangular shape, size  $6 \times 6 \times 100 \text{ mm}$ , with a volume of ca.  $3 \text{ cm}^3$ . The total volume of the glass dilatometer was about  $8 \text{ cm}^3$ . For the aging measurements three thermostatic baths were used, two filled with silicon oil for higher temperatures and one with water of room temperature. The annealing procedure, during which the possible thermal or mechanical histories were erased, was performed in the first bath. Then the MIG dilatometer was manually transferred to the second thermostating bath of the relaxation temperature. They were of two types: one with temperature stability  $\pm 0.01^\circ\text{C}$ , which was used for PMMA and PC, and the other with stability  $\pm 0.02^\circ\text{C}$  for a-Se. The accuracy of volume measurements was assessed from the smallest measurable volume changes together with temperature fluctuation of the particular bath according to its temperature stability. These values differ for various dilatometers because of the differences in dilatometer's parameters, such as the capillary diameter, amount of mercury, kind, and amount of the sample. The calculated values for each dilatometer were  $\pm 1.3 \times 10^{-5} \text{ cm}^3/\text{cm}^3$  for the dilatometer filled with a-PMMA,  $\pm 2.0 \times 10^{-5} \text{ cm}^3/\text{cm}^3$  for the PC-filled dilatometer, and  $\pm 1.9 \times 10^{-5} \text{ cm}^3/\text{cm}^3$  for the dilatometer with a-Se. These values belong to systematic errors of this type of volume relaxation measurements. The analysis of random errors was not possible because each experiment was only performed once. This is quite common in the research field in question as the experiments are extremely time demanding.

For the *enthalpic* experiments differential scanning calorimetry (DSC) was used. The samples for DSC analyses weighed ca. 6mg and were sealed in an aluminum pan. For the measurements performed at ambient temperature on a-Se, an intracooler was used. The temperature and heat flow of DSC were calibrated on heating

at 10°C/min using indium standard. The change in enthalpy during relaxation was determined by the difference in the areas under the aged and unaged sample scans. Both curves were integrated between temperatures where the curves overlap the instrument baseline. The procedure assumes that the same degree of relaxation occurs during cooling for both the aged and unaged samples. One disadvantage of this method is a large variation in the values of  $\Delta h$  obtained in measurements by different investigators, which results from the difficulty in determining the points of deviation from the sample baseline [21].

An extensive analysis of systematic errors of enthalpy relaxation measurements was done. The standard deviations of relaxation for the same experimental condition calculated from the set of ten experiments performed as intrinsic cycles was  $\pm 0.012$  J/g for the amount of relaxed enthalpy (evaluated as a peak area),  $\pm 0.023$  °C for the onset of glass transition temperature, and  $\pm 0.011$  °C for the peak temperature (maximum).

Experimental conditions used during the annealing, cooling/heating, and aging stages are specified in the following sections.

Aging bulk moduli were calculated as a slope of the  $\Delta h/\Delta v$  dependence. A satisfactorily linear graph was achieved for each material. The standard deviation was calculated as a lower and upper bounds on  $K$  parameter computed with the help of Student  $t$  distribution, probability of error  $\alpha = 0.005$ . The calculated values are presented in appropriate figures as error bars.

### 3. Results

The research results will be presented from various points of view: temperature jumps, materials, and cooling rates.

#### 3.1. Temperature down-jumps (PMMA, PC)

The aging data measured on PMMA was obtained in two series of experiments. In the first one the sample was kept at 6°C above aging temperature ( $T_a$ ), then cooled to  $T_a$ , and enthalpy and volume relaxation was recorded. In the second series the temperature down-jump to various  $T_a$ s was done from an annealing temperature of  $T_{g,enth.} + 20^\circ\text{C}$ . The obtained  $K_a$  values were largely similar in both types of experiments. In order to assess the quality of  $K_a$  data extracted from  $h(v)$  plots, Fig. 1 shows the kinetics of the enthalpy and volume relaxation process in PMMA with the thermal history specified in Scheme 1.

With regard to enthalpy measurements, the data given in the scheme need clarification. Obviously, using DSC device becomes impractical when longer aging periods,  $t_a$ , are considered. Thus, in the experiments

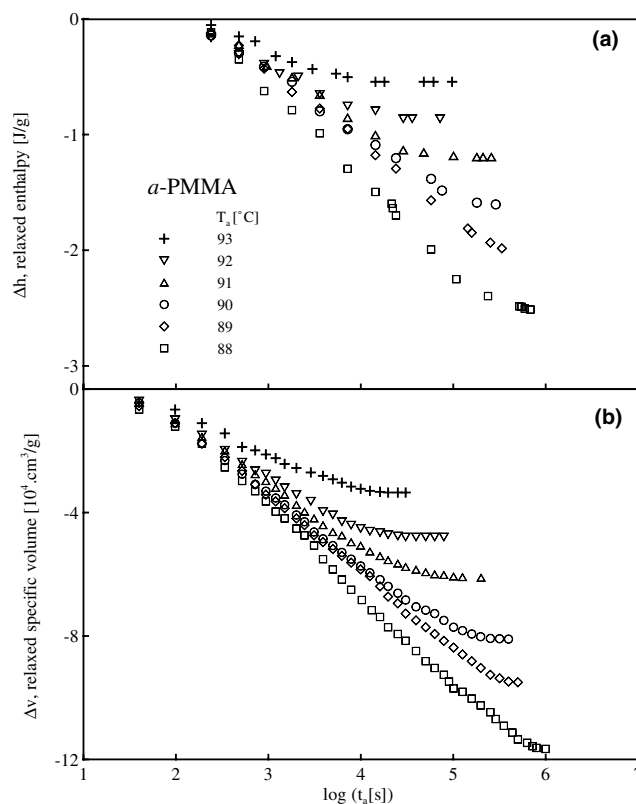
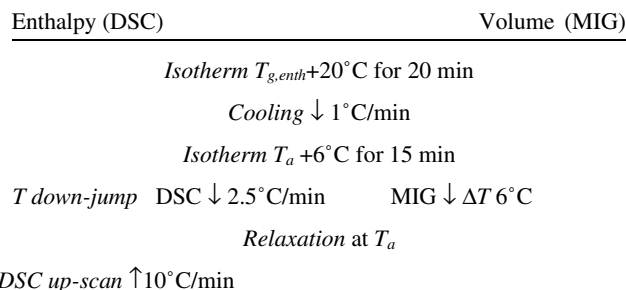


Fig. 1. Enthalpy (a) and volume (b) relaxation curves for a-PMMA after temperature down-jumps to different aging temperatures,  $T_a$ , from  $T_a + 6^\circ\text{C}$ .



Scheme 1. Thermal history of a-PMMA ( $T_{g,enth.} = 95^\circ\text{C}$ ), and PC ( $T_{g,enth.} = 145^\circ\text{C}$ );  $T$  down-jump of  $6^\circ\text{C}$  to various  $T_a$ s.

the samples were kept in DSC not more than half an hour. For longer aging they were transferred to a precision bath held at  $T_a$ , where they were kept in a thin-walled Al tube, for the rest of the aging period. Then the tested sample was transferred back to DSC device for the  $T$  up-scan, which started at a temperature of  $T_{g,enth.} - 55^\circ\text{C}$ . This procedure thus implies that during the transfer of the sample the aging process was under unidentified conditions (lower  $T_a$ ) for some 10–20 s. However, the above procedure did not influence the final results, as could be seen in comparable control tests.

A common feature of the  $h(\log t)$  and  $v(\log t)$  dependences in Fig. 1 is the same size of the  $T$  down-jump, that is  $6^\circ\text{C}$ , to a specific aging temperature. In the volumetric measurements this change was realized by transferring the MIG device to a precision bath of a temperature  $6^\circ\text{C}$  lower than the bath where the sample was annealed. The average cooling rate resulting from this transfer was estimated at  $2.5^\circ\text{C}/\text{min}$ . In order to maintain similar conditions also in the enthalpic experiments, the same cooling rate was used when approaching  $T_a$  in the DSC device. In principle, the somewhat unusual cooling scheme selected here is equivalent to the changing difference in  $T_{g,\text{enth.}} - T_a$ . This is also clearly reflected in the extent of relaxation of both enthalpy and volume. In the  $\log t$  dependence in Fig. 1 we find the usual sigmoid shape with a clearly visible approach to equilibrium, at least at the higher  $T_a$  levels.

It may be added that the first volume reading on the MIG device was done 140 s after the sample transfer to the  $T_a$  bath. In this way the initial steep fall in volume due to temperature equilibration was eliminated. This procedure, however, does not influence the magnitude of  $K_a$ , which is determined by volume differences and not by the actual volume.

Generally, when plotting relaxed enthalpy vs. relaxed volume, we obtain a basically linear graph. This is also true for a-PMMA in our case, Fig. 2(a). A more detailed view can be seen in the remaining three parts of the figure presenting the data measured for particular aging temperatures. The line shown in all four parts of Fig. 2 was obtained by regression including all the measured points. There is no significant deviation from this line at any  $T_a$ . The  $K_a$  values for various  $T_a$ s range from 2.23 to 2.57 GPa.

Polycarbonate (PC),  $T_{g,\text{enth.}} = 145^\circ\text{C}$ , showed largely similar results to those shown above for a-PMMA for the same temperature down-jump (from  $T_a + 6^\circ\text{C}$  to  $T_a$ ). Also PC behavior under the other conditions was anal-

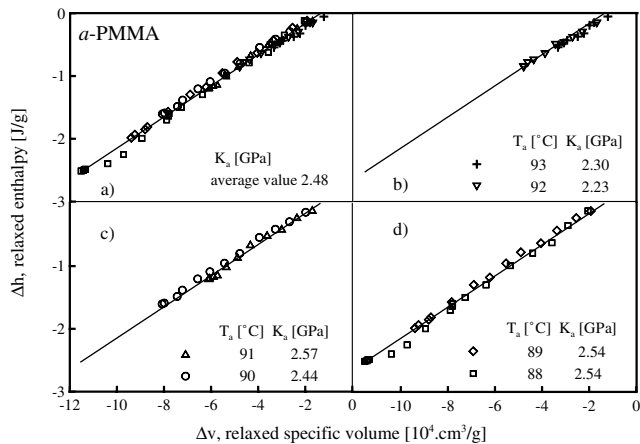


Fig. 2. Aging bulk moduli,  $K_a$ , calculated from enthalpy and volume relaxation data of a-PMMA, Fig. 1.

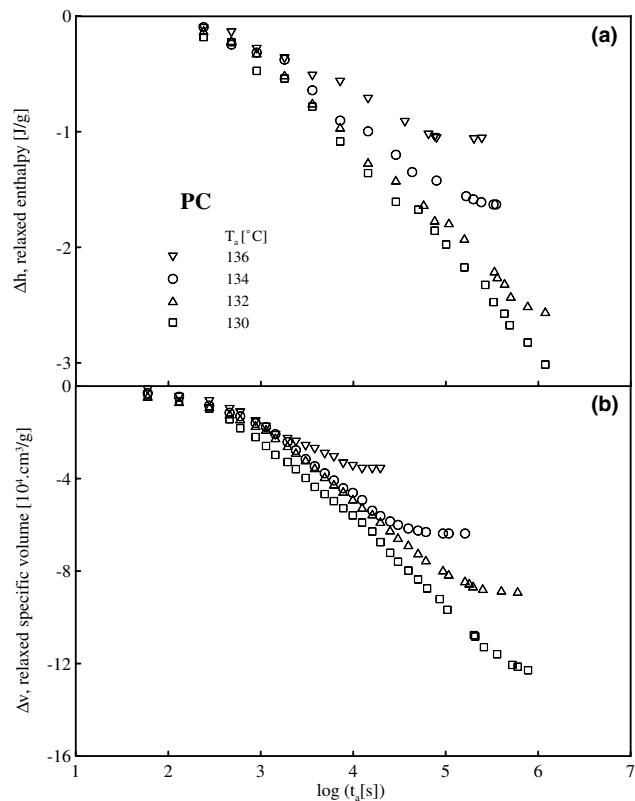


Fig. 3. Enthalpy (a) and volume (b) relaxation curves for PC after temperature down-jumps to different aging temperatures,  $T_a$ , from  $T_a + 6^\circ\text{C}$ .

ogous to a-PMMA. Fig. 3 shows the enthalpy and volume relaxation. As in the previous case, the preciseness of relaxed-volume data is better than that of relaxed enthalpy. Another difference between the two graphs is the faster approach of the volume toward equilibrium, i.e. the shift of these curves to shorter times. The thermal history of the samples before reaching  $T_a$  was the same as described above for a-PMMA, including the  $T$  down-jump of  $6^\circ\text{C}$  to  $T_a$  from the annealing temperature (Scheme 1).

The data for PC from the previous part were plotted in one graph, and are displayed in Fig. 4. Since the data was obtained at four  $T_a$ s only, no conclusions can be made about possible  $K_a(T_a)$  dependence. The  $K_a$  values range from 2.0 to 2.3 GPa, thus paralleling the data on PMMA.

As already mentioned, the kinetics of the volumetric and enthalpic approach to equilibrium exhibits some differences (Figs. 1 and 3). First of all, the equilibrium state of the  $v(\log t)$  curves is reached prior to that of the corresponding enthalpy graphs. Due to this, the  $h(v)$  plots, from which  $K_a$  is calculated, cannot be expected to take a linear course in the final stage of aging process, where enthalpy continues to decrease while the volume only shows a minute change. This, in turn, results in a sharp increase of  $K_a$ , which justifies the exclu-

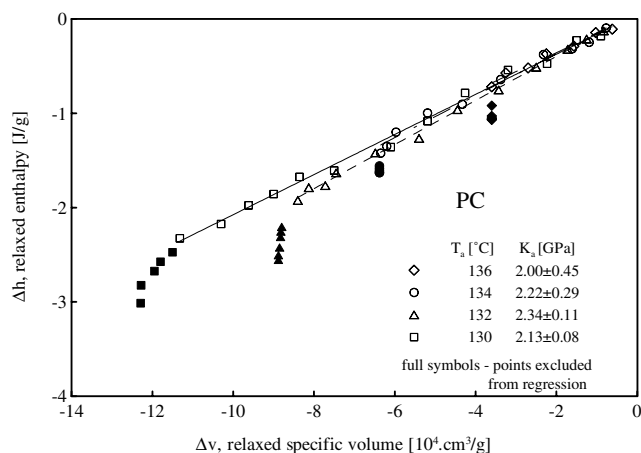


Fig. 4. Aging bulk moduli,  $K_a$ , calculated from enthalpy and volume relaxation data of PC, Fig. 3.

sion of such data from the construction of  $h(v)$  regression lines, as indicated in Fig. 4. No such deviations were noted in the initial stage, where the first readings relate to the linear portion of the  $\log t$  plots of  $h$  and  $v$ .

In the second series of aging measurements on PMMA the specimen was cooled from  $T_{g,enth.} + 20^\circ\text{C}$  to different levels of  $T_a$  (95, 89, 86, 81, and  $73^\circ\text{C}$ ) according to Scheme 2. Unlike in the previous case the sample stayed in the DSC device during the whole measurement including the aging period. While in the enthalpic tests the cooling rate of the sample was  $10^\circ\text{C}/\text{min}$ , the rate of volumetric aging in the MIG dilatometer was determined by the difference between  $T_{g,enth.} + 20^\circ\text{C}$  and  $T_a$ . Although the rate in the two cases may be similar in the order of magnitude, a perfect match is difficult to achieve, not the least due to the widely dissimilar size of the samples and the resulting difference in temperature equilibration.

The time dependent relaxed volume and enthalpy obtained from Scheme 2 aging process are shown in Fig. 5. The enthalpic data was recorded within a relatively narrow time window, corresponding approximately to the linear portion of  $v(\log t)$ . In contrast to Fig. 1, where the slope of the latter graphs and also the extent of the volume change were related to  $T_a$ , this is not so in the present case, apparently due to the saturation effect indicating significant deviation from linear behavior.

Enthalpy (DSC)	Volume (MIG)
Isotherm $T_{g,enth.}+20^\circ\text{C}$ for 20 min	
$T$ down-jump	DSC $\downarrow 10^\circ\text{C}/\text{min}$ MIG $\downarrow \Delta T = T_a - (T_{g,enth.}+20^\circ\text{C})$
Relaxation at $T_a$	
DSC up-scan $\uparrow 10^\circ\text{C}/\text{min}$	

Scheme 2. Thermal history of a-PMMA ( $T_{g,enth.} = 95^\circ\text{C}$ ); cooling from  $T_{g,enth.} + 20^\circ\text{C}$  to various  $T_a$ s.

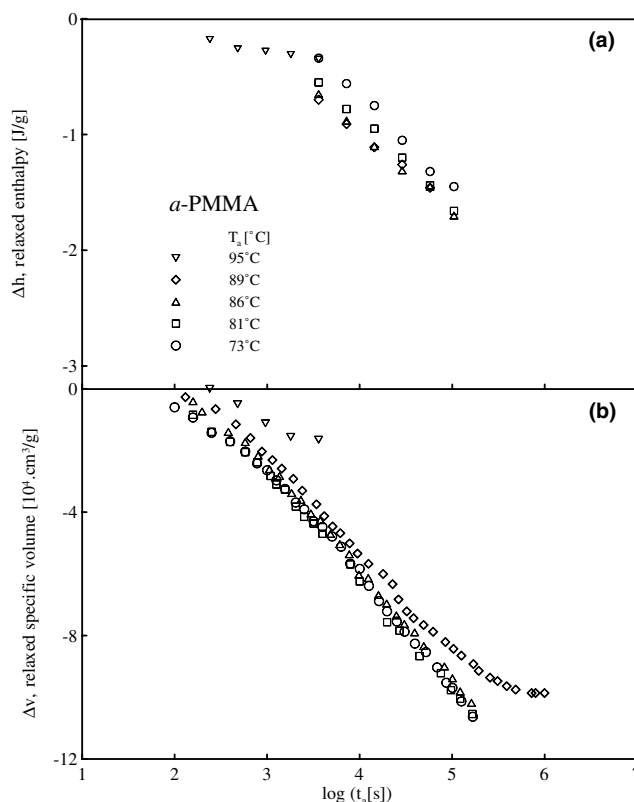


Fig. 5. Enthalpy (a) and volume (b) relaxation curves for a-PMMA after temperature down-jump to different aging temperatures,  $T_a$ , from  $T_{g,enth.} + 20^\circ\text{C}$ .

Such an effect is well known from earlier studies [22,23]. In our case this effect seems to be caused by the positional closeness of the volumetric data. Exceptions to this pattern are the  $h$  and  $v$  relaxation curves relating to  $T_{g,enth.} = T_a = 95^\circ\text{C}$ . Their limited extent, however, does not allow any comparison with the rest of the data.

When plotting the relaxed quantities  $h$  and  $v$  from Fig. 5 against each other, we obtain the graphs shown in Fig. 6, yielding  $K_a$  of 1.8–2.1 GPa. The  $K_a$  value at  $T_a = T_{g,enth.}$ , i.e. 0.93 GPa, is not included in this range as  $T_{g,enth.}$  and  $T_a$  practically do not differ. This can be justified by the course of underlying kinetics shown in Fig. 5 for  $95^\circ\text{C}$  (for the minute changes the material gets into the equilibrium state very fast).

### 3.2. Temperature up-jumps (PMMA)

Aging moduli can also be determined from aging data recorded after a stepwise increase in temperature from  $T_{a1}$  to  $T_{a2}$ , where  $T_{a1} < T_{a2} < T_g$ . In these experiments the volume and enthalpy increase during the aging process. The aging kinetics of a-PMMA after a temperature up-jump is shown in Fig. 7, and the thermal history is specified in Scheme 3. For comparison, a curve of down-jump schedule is also given (full symbols). The

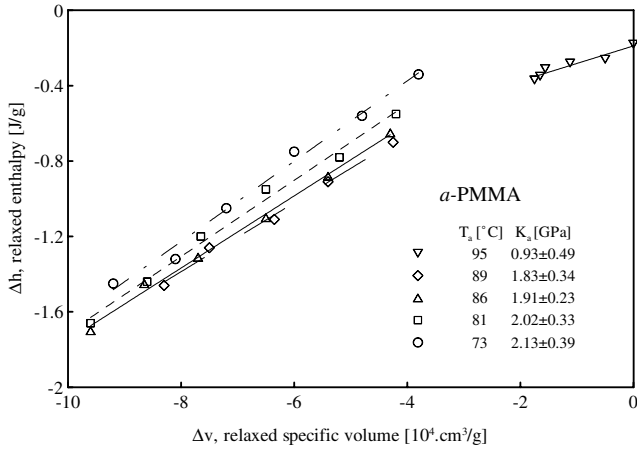


Fig. 6. Aging bulk moduli,  $K_a$ , calculated from enthalpy and volume relaxation data of a-PMMA, Fig. 5.

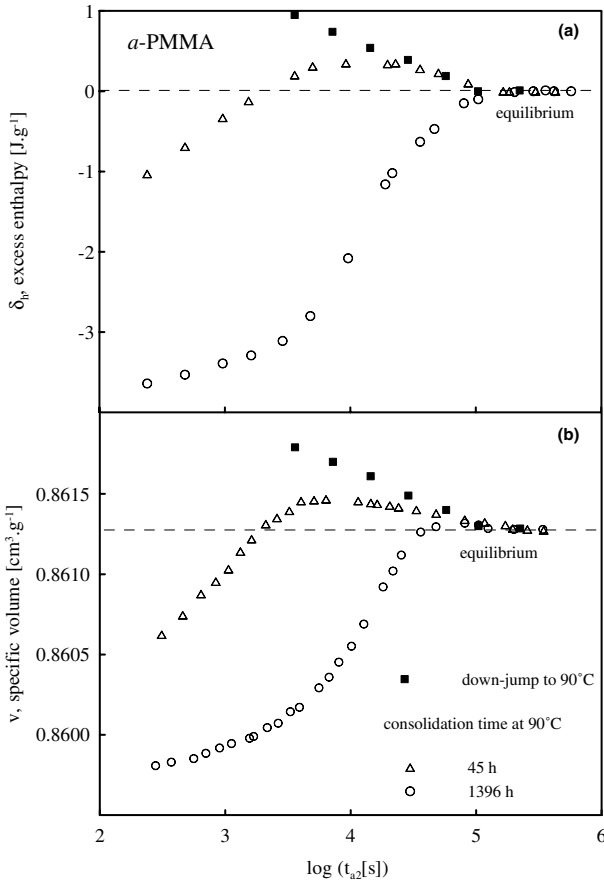


Fig. 7. Enthalpy (a) and volume (b) relaxation data for a-PMMA after  $T$  down- and up-jumps to  $T_{a2} = T_{g,enth.} - 5^\circ\text{C} = 90^\circ\text{C}$ .

graph shows the commonly observed asymmetry of the approach to equilibrium following cooling and heating [24]. When interpreting the kinetics in terms of relaxation times spectrum, one finds a significantly narrower range in the latter case (Fig. 7), almost a single exponen-

Enthalpy (DSC) Volume (MIG)

---

*Isotherm  $T_{g,enth}+20^\circ\text{C}$  for 20 min*

*$T$  down-jump to  $T_{a1} = T_{g,enth.} - 15^\circ\text{C} = 80^\circ\text{C}$*

*Consolidation at  $T_{a1}$  up to 1396 h*

*$T$  up-jump to  $T_{g,enth.} - 5^\circ\text{C} = 90^\circ\text{C} \uparrow 3^\circ\text{C}/\text{min}$*

*Relaxation at  $T_{a2}$*

*DSC up-scan  $\uparrow 10^\circ\text{C}/\text{min}$*

Scheme 3. Thermal history of a-PMMA ( $T_{g,enth.} = 95^\circ\text{C}$ ),  $T$  up-jump from  $T_{a1} = 80^\circ\text{C}$  to  $T_{a2} = 90^\circ\text{C}$ .

tial, at least when the process starts from a state close to equilibrium. When the  $T$  up-jump is done from a not completely relaxed state, the sample remembers its cooling history, showing memory effects analogous to similar viscoelastic phenomena (e.g. [5]). As can be seen, both enthalpy and volume reach a maximum (overshoot) before approaching their equilibrium values. The shorter the consolidation time at temperature  $T_{a1}$ , the more pronounced this effect is. Remarkable is also the fact that the final part of the up-jump curves at equilibrium coincides with the aging curve from a down-jump to the same  $T_a$ , which supports the idea that the equilibrium is the same regardless the temperature direction from which it is reached.

Plotting both sets of data in one graph, the magnitudes of  $K_a$  were obtained again. As evident from Fig. 8, the values are similar to those in  $T$  down-jump measurements. The enthalpy vs. volume plots shown here were assembled from  $T$  up-jump data after 45 and 1396 h consolidation time at  $T_{a1}$  ( $80^\circ\text{C}$ ), before increasing the temperature to  $T_{a2}$  ( $90^\circ\text{C}$ ). The latter  $T_a$  value

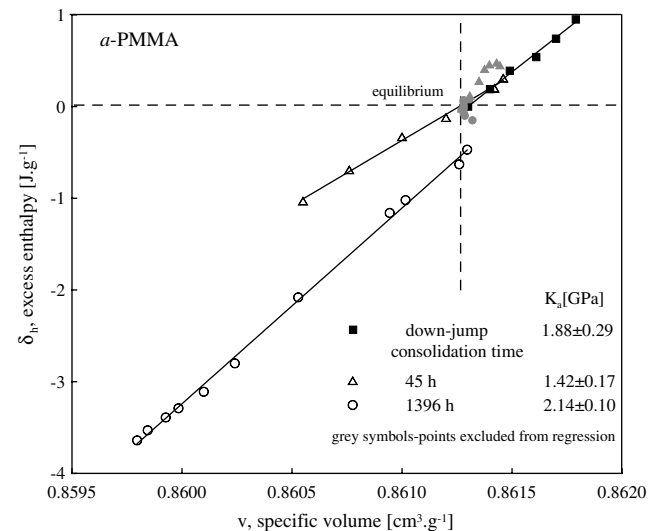


Fig. 8. Aging bulk moduli,  $K_a$ , calculated from enthalpy and volume relaxation data for down- and up-jumps to  $T_a = T_{g,enth.} - 5^\circ\text{C} = 90^\circ\text{C}$ , a-PMMA.

was also used in the down-jump (from  $T_{g,enth.} + 20^\circ\text{C}$ ) measurements. As can be seen, all three plots are fairly linear. The slope of the line obtained after 45 h consolidation time at  $80^\circ\text{C}$  is lower than that of the line measured after 1396 h. One may also note that the  $\delta_h/v$  lines do not cross line  $\delta_h = 0$  at the same point when approaching it from below and from above directions. In accordance with [6]  $K_a$  values are slightly larger after a positive  $T$  change than after a negative one, Fig. 8. An interesting feature of the graphs in this figure is their linearity, not only of the down-jump results, but also the data from the up-jump experiments, where the underlying  $h(\log t)$  and  $v(\log t)$  curves show a distinctly non-linear (sigmoid) shape (Fig. 7). In the latter measuring mode,  $K_a$  is normally evaluated from the linear portion of the curve. As can be seen in Fig. 8, the  $\delta_h/v$  line for the sample consolidated for 45 h continues beyond the equilibrium values of both  $h$  and  $v$  without changing its slope. This line includes data up to the maximum of their equilibrium overshoot, cf. Fig. 7. The points marking the return from the maximum to equilibrium form a loop in the  $\delta_h(\Delta v)$  graph; they were excluded from the regression line. The data in Figs. 7 and 8 have been adapted from Ref. [24], where a more detailed description of the experimental procedure can be found. The relation between  $K_a$  and compressibility, which is the aim of the present paper, will be presented in the Discussion section.

### 3.3. Influence of cooling rate (PMMA)

One of the key factors determining the kinetics of the aging process as well as its magnitude is the difference between glass transition temperature,  $T_g$ , and aging temperature,  $T_a$ . However, while  $T_a$  can be kept constant during the measurement, the actual  $T_g$  value depends on the rate of cooling. This leads to complications, especially in MIG-type experiments, where, due to the size of the sample, the temperature gradient apparently influences structural consolidation. In our research we wanted to assess, at least qualitatively, the possible influence of cooling rate on the behavior of PMMA after temperature down-jumps. Three cooling rates were selected for DSC: 2.5, 10, and  $20^\circ\text{C}/\text{min}$ . The detailed schedule of the test is specified in Scheme 4. For MIG

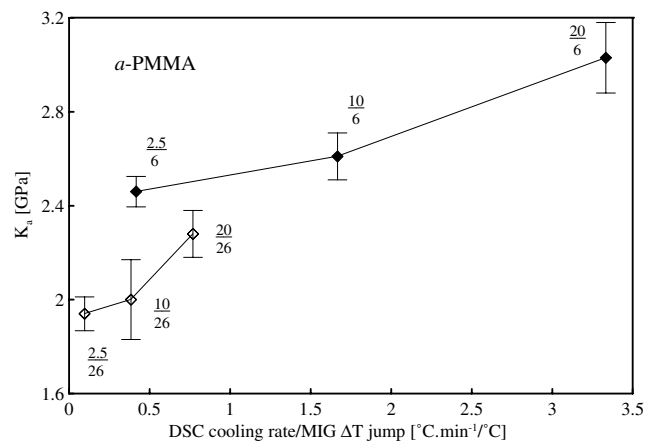


Fig. 9. Dependence of  $K_a$  on the DSC cooling rate/MIG  $\Delta T$  jump, a-PMMA,  $T_a = 89^\circ\text{C}$ .

the estimated average cooling rates were about  $2.5$  and  $10^\circ\text{C}/\text{min}$ . Omitting the underlying primary data, in Fig. 9 we show a graphical representation of the dependence of  $K_a$  on cooling rate. For the different modes two graphs were obtained where an increase in  $K_a$  with cooling rate in DSC measurements is evident. However, as the results only have a qualitative character we refrain here from a closer discussion. It may suffice to note that at constant  $\Delta T$  the increase with DSC cooling rate is apparently caused by the corresponding rise in  $T_{g,enth.}$ , and thus by an overall larger enthalpy relaxation.

### 3.4. Measurements on amorphous selenium

To compare the aging properties of amorphous polymers with those of inorganic glass we chose a-Se. The main idea was to prove whether also here any relation between  $K_a$  and  $\kappa$  exists. (For Se the value of  $\kappa$  is significantly lower than that for organic polymers.) Fig. 10 shows enthalpy and volume aging results obtained in measurements. The thermal history of the sample was basically the same as in the case of PMMA, and is specified in Scheme 5; both  $T$  up- and down-jumps were recorded. The data shown in Fig. 10 exhibits the usual features of enthalpy and volume relaxation, including the asymmetry of the  $\log t$  graphs when approaching  $T_a$  from higher and lower temperatures. Despite this asymmetry, these graphs seem to reach the equilibrium line at roughly the same time, independent of the direction in which  $h$  or  $v$  are approaching. The corresponding  $\Delta h(\Delta v)$  plots are displayed in Fig. 11. Again, we obtain a fairly linear dependence of these quantities, yielding  $K_a$  values of around  $5.8$  and  $4.8$  GPa in the down-jump and up-jump modes, respectively. In contrast to PMMA we thus find here a lower value for temperature up-jump.

Enthalpy (DSC)	Volume (MIG)
	Isotherm $T_{g,enth.}+20^\circ\text{C}$ for 20 min
	Cooling to $T_{g,enth.}+6^\circ\text{C} \downarrow 1^\circ\text{C}/\text{min}$
Isotherm $T_{g,enth.}+20^\circ\text{C}$ for 20 min	$T_{g,enth.}+6$ and $+20^\circ\text{C}$ for 20 min
$T$ down-jump DSC $\downarrow 20, 10$ and $2.5^\circ\text{C}/\text{min}$	MIG $\downarrow \Delta T = T_a - (T_{g,enth.}+6$ and $+20^\circ\text{C})$
	Relaxation at $T_a$
DSC up-scan $\uparrow 10^\circ\text{C}/\text{min}$	

Scheme 4. Thermal history of a-PMMA ( $T_{g,enth.} = 95^\circ\text{C}$ ), different cooling rates.



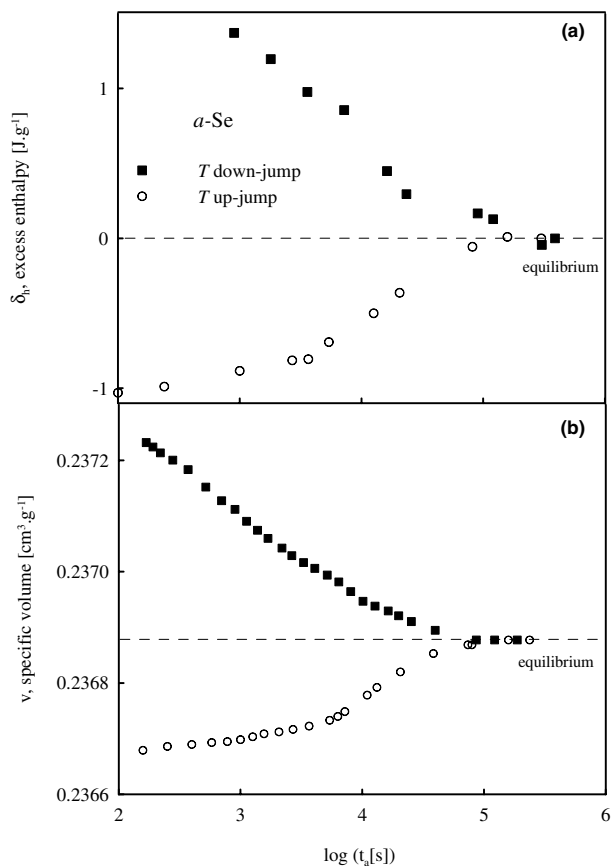


Fig. 10. Enthalpy (a) and volume (b) relaxation data for a-Se after  $T$  down- and up-jumps to  $T_a = T_{g,enth.} - 10^\circ\text{C} = 28^\circ\text{C}$ .

Enthalpy (DSC)		Volume (MIG)
<i>Isotherm <math>T_{g,enth}+10^\circ\text{C}</math> for 30 min</i>		
<i>T down-jump</i>	DSC $\downarrow 10^\circ\text{C}/\text{min}$	MIG $\downarrow \Delta T 20^\circ\text{C}$
	<i>to <math>T_{a1} = T_{g,enth.} - 10^\circ\text{C} = 28^\circ\text{C}</math></i>	
	<i>Consolidation at <math>T_{a1}</math> for 200 h</i>	
	<i>T up-jump to <math>T_{g,enth} - 5^\circ\text{C} = 33^\circ\text{C}</math></i>	
	<i>Relaxation at <math>T_{a2}</math></i>	
	<i>DSC up-scan <math>\uparrow 10^\circ\text{C}/\text{min}</math></i>	

Scheme 5. Thermal history of a-Se ( $T_{g,enth.} = 38^\circ\text{C}$ ),  $T$  up-jump from  $T_{a1} = 28^\circ\text{C}$  to  $T_{a2} = 33^\circ\text{C}$ .

Shifting the experimental temperature region to lower values, we can see a decrease in  $K_a$ , as shown in Fig. 11 for a  $T$  down-jump to  $T_a = 23^\circ\text{C}$  ( $K_a = 4.93$  GPa).

#### 4. Discussion

The data obtained in Section 3 was the base for setting the relation between  $K_a$ , i.e.  $\Delta h/\Delta v$ , and the mate-

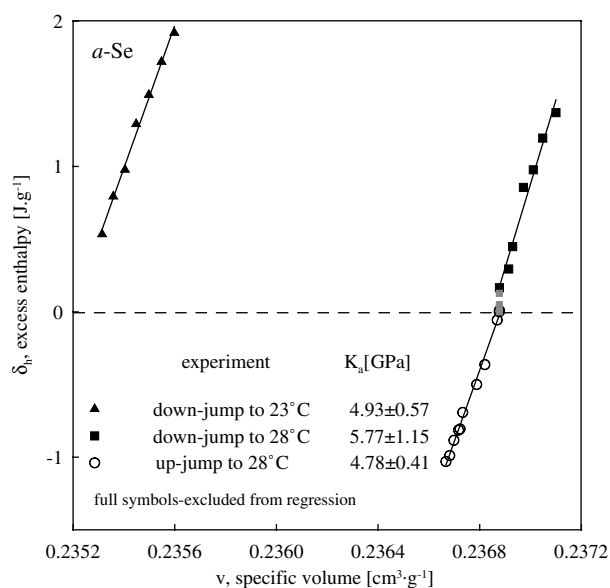


Fig. 11.  $K_a$  for a-Se calculated from  $T$  down- and up-jumps to  $T_a = T_{g,enth.} - 10^\circ\text{C} = 28^\circ\text{C}$  from the data in Fig. 10, and  $K_a$  determined from down-jump measurements to  $T_a = T_{g,enth.} - 15^\circ\text{C} = 23^\circ\text{C}$ .

rial's compressibility. To enlarge the validity of such relation beyond common amorphous polymers (PMMA, PC), also an inorganic glassy material (a-Se) was included.

Since aging measurements are normally carried out close to  $T_g$ , it appears natural to compare the values of  $\Delta h/\Delta v$  with  $1/\kappa_1$ , that is the inverse of the compressibility above  $T_g$  (in the index 1 means liquid). Normally, the variation between compressibility of glassy and liquid state of the material is not taken into account, which is also sufficient for our present purpose. In Ref. [25] the inverse  $\kappa_1$  values for common amorphous polymers are about 2 GPa, corresponding to  $\kappa_1$  between 40 and 60 in  $10^{-5}\text{MPa}^{-1}$ . For the PMMA grade used in our measurements Schmidt and Maurer [26] obtained a  $\kappa_1$  value of  $44.4 \times 10^{-5}\text{MPa}^{-1}$ , corresponding to bulk modulus  $K_1 = 2.25$  GPa ( $pvT$  device, isothermal mode). Similar values also appear in other references given above.

Unlike for amorphous organic polymers the values of  $1/\kappa$  for a-Se are lower by a factor of 2–3. The fair agreement between our  $\Delta h/\Delta v$  data and the bulk modulus values extracted from  $pvT$  measurements by Berg and Simha [27] supports the notion that  $\Delta h/\Delta v$  indeed is closely related to  $1/\kappa$  at the upper end of the  $T_g$  region. The bulk modulus presented in the mentioned paper is about 6 GPa, while the range of our  $\Delta h/\Delta v$  results is 4.5 to 5.8 GPa.

It should be noted that the data given in the present paper account only for a part of an experimental investigation aiming at the evaluations of the  $\Delta h/\Delta v$  ratio from enthalpy and volume relaxation records. In general, there is a fairly solid support for the idea that  $K_a$

is close to the inverse of  $\kappa_1$  extracted from  $pVT$  measurements, as also supported by our results.

The reader may note that the measurement results depend not only on temperature but also a number of other factors; they are therefore not to be considered as constants characterizing the state of a given material. Nevertheless, the similar magnitude of  $\Delta h/\Delta v$  and  $1/\kappa_1$  seems to offer a possibility to consider the enthalpy relaxation process as a result of the dissipation of frozen-in  $pV$  work.

## 5. Conclusions

Volume and enthalpy relaxation data recorded during physical aging of PMMA and PC confirm that the aging modulus,  $K_a$ , defined in a tentative manner as  $\Delta h/\Delta v$ , tends to assume values close to the inverse value of the compressibility,  $1/\kappa_1$ , around  $T_g$ , i.e. about 2 GPa. The notion that  $K_a$  is of similar magnitude as  $1/\kappa_1$  is supported by measurements on amorphous selenium, which has a significantly lower compressibility than the common amorphous polymers above.

Aging experiments in the  $T$  up- and down-jump modes yield slightly different results for  $K_a$ , so the approach to the equilibrium state from different temperature directions is asymmetric. Another factor influencing  $K_a$  is the rate of cooling/heating, which appears to be related to the corresponding changes in  $T_g$ .

## Acknowledgments

The financial support of the Czech Ministry of Education, project MSM 265200015, and Czech Science Foundation, project GAT 31580, is gratefully acknowledged. One of the authors (PŘ) wishes to express his thanks to the Grant Agency of the Academy of Science of the Czech Republic for grant no. A2060401. We would also like to thank Pavla Pustková, MSc, University of Pardubice, Czech Republic, for kindly providing the a-Se specimen. Special thanks are due to Professor

Lennart Sjögren, Department of Theoretical Physics, Chalmers University of Technology, Gothenburg, Sweden, for his valuable help with the calculations based on Nieuwenhuizen's approach.

## References

- [1] L.C.E. Struik, Physical aging of amorphous polymers and other materials, Elsevier, Amsterdam, 1978.
- [2] G.B. McKenna, in: C. Booth, D. Price (Eds.), Comprehensive Polymer Science, Polymer Properties, vol. 2, Pergamon, Oxford, 1989, p. 311.
- [3] J.M. Hutchinson, Prog. Polym. Sci. 20 (1995) 703.
- [4] C.A. Angell, K.L. Ngai, G.B. McKenna, P.F. McMillan, S.W. Martin, J. Appl. Phys. 88 (2000) 3113.
- [5] K. Adachi, T. Kotaka, Polym. J. 14 (1982) 959.
- [6] E.O. Oleinik, Polym. J. 19 (1987) 105.
- [7] S.L. Simon, D.J. Plazek, J.W. Sobieski, E.T. McGregor, J. Polym. Sci., Part B: Polym. Phys. 35 (1997) 929.
- [8] S.L. Simon, J.W. Sobieski, D.J. Plazek, Polymer 42 (2001) 2555.
- [9] J.M.G. Cowie, S. Harris, I.J. McEwen, Macromolecules 31 (1998) 2611.
- [10] M.J. Kubát, J. Vernel, R.W. Rychwalski, J. Kubát, Polym. Eng. Sci. 38 (1998) 1261.
- [11] R.O. Davies, G.O. Jones, Adv. Phys. 2 (1953) 370.
- [12] R.O. Davies, G.O. Jones, Proc. Roy. Soc. London. A 217 (1953) 26.
- [13] A.J. Staverman, Rheol. Acta 5 (1966) 283.
- [14] G. Rehage, J. Macromol. Sci.: Phys. B 18 (1980) 423.
- [15] R.J. Speedy, J. Phys. Chem. B 103 (1999) 8128.
- [16] J. Wu, J. Appl. Polym. Sci. 71 (1999) 143.
- [17] Th.M. Nieuwenhuizen, J. Phys.: Condens. Matter. 12 (2000) 6543.
- [18] Th.M. Nieuwenhuizen, Phys. Rev. E 61 (2000) 267.
- [19] H. Baur, Thermodynamics of Polymers, 1. Theory, Springer, 1999, p. 197.
- [20] S. Schantz, Macromolecules 30 (1997) 1419.
- [21] T. Hatakeyama, F.X. Quinn, Thermal Analysis—Fundamental and Applications to Polymer Science, John Wiley and Sons, West Sussex, 1994.
- [22] J. Málek, S. Montserrat, Thermochim. Acta 313 (1998) 191.
- [23] R. Greiner, F.R. Schwarzl, Rheol. Acta 23 (1984) 378.
- [24] P. Slobodian, A. Lengálová, P. Sába, JTAC 71 (2003) 387.
- [25] J.M. O'Reilly, J. Appl. Phys. 48 (1977) 4047.
- [26] M. Schmidt, F.H.J. Maurer, J. Polym. Sci. B: Polym. Phys. 36 (1998) 1061.
- [27] J.I. Berg, R. Simha, J. Non-Cryst. Solids 22 (1976) 1.